http://doi.org/10.35784/iapgos.7518 received: 10.04.2025 | revised: 23.09.2025 | accepted: 18.11.2025 | available online: 20.12.2025

STOCHASTIC MULTI-OBJECTIVE MINIMAX OPTIMIZATION OF COMBINED ELECTROMAGNETIC SHIELD BASED ON THREE-DIMENSIONAL MODELING OF OVERHEAD POWER LINES MAGNETIC FIELD

Borys Kuznetsov[1], Tatyana Nikitina[2], Alexander Kutsenko[1], Ihor Bovdui[1], Kostiantyn Chunikhin[1], Olena Voloshko[1], RomanVoliansky[3], Viktoriia Ivannikova[4]

[1]Anatolii Pidhornyi Institute of Power Machines and Systems of the National Academy of Sciences of Ukraine, Department of Magnetism of Technical Objects, Kharkiv, Ukraine, [2]Bakhmut Education Research and Professional Pedagogical Institute V. N. Karazin Kharkiv National University, Electromechanical and Computer Systems Department, Bakhmut, Ukraine, [3]National Technical University of Ukraine "Igor Sikorsky Kyiv Polytechnic Institute", Department of Electromechanical Systems Automation and Electrical Drives, Kyiv, Ukraine, [4]National Aviation University, Air Navigation Systems Department, Kyiv, Ukraine

Abstract. *The method of design of combined electromagnetic shield, consisting from active shielding system and electromagnetic passive shield of overhead power lines magnetic field is developed. All designed parameters calculated as multi-objective nonlinear minimax optimization problem solution based on stochastic particles multi-swarm optimization algorithms. Vector nonlinear objective function calculated based on finite element calculations system COMSOL Muliphysics package. Theoretical and experimental studies results of designed combined electromagnetic shield are presented.*

Keywords: combined electromagnetic shield, three-dimensional modeling, stochastic multi-objective minimax optimization, modeling and experimental studies

STOCHASTYCZNA WIELOCELOWA OPTYMALIZACJA MINIMAKSOWA POŁĄCZONEGO EKRANU ELEKTROMAGNETYCZNEGO W OPARCIU O TRÓJWYMIAROWE MODELOWANIE POLA MAGNETYCZNEGO NAPOWIETRZNYCH LINII ELEKTROENERGETYCZNYCH

Streszczenie. *Opracowano metodę projektowania kombinowanej osłony elektromagnetycznej, składającej się z aktywnego systemu ekranującego i pasywnej osłony elektromagnetycznej pola magnetycznego napowietrznych linii energetycznych. Wszystkie parametry projektowe obliczono jako rozwiązanie wielokryterialnego nieliniowego problemu optymalizacji minimaksowej w oparciu o stochastyczne algorytmy optymalizacji wieloprzestrzennej cząstek. Nieliniową funkcję celu wektorowego obliczono w oparciu o system obliczeń elementów skończonych pakietu COMSOL Muliphysics. Przedstawiono wyniki badań teoretycznych i eksperymentalnych zaprojektowanej kombinowanej osłony elektromagnetycznej.*

Słowa kluczowe: połączona osłona elektromagnetyczna, modelowanie trójwymiarowe, stochastyczna wielokryterialna optymalizacja minimaksowa, modelowanie i badania eksperymentalne

Introduction

Many residential buildings located in close proximity to overhead power lines (OPL). Power frequency (PF) magnetic field induction level in such buildings is many times higher than modern standards for PF MF induction level for population living safe [10, 14, 15]. One of most economically justified approaches to further operation of high-grade residential buildings without eviction of population or replacement of existing OPL with underground cable power lines used of MF shielding to safe level for habitation [9, 11]. To increase effectiveness of shielding, especially in long-distance residential buildings, it is advisable used MF combined electromagnetic shield (CES), consisting from system of active shielding (SAS) and electromagnetic passive shield (EPS) [7].

This research contributes to development method for improvement effectiveness of OPL PF MF reduction by CES, consisting from SAS and EPS, based on three-dimensional modelling (TDM) and taking into account reduction effectiveness of original OPL PF MF shielding at residential building edges (RBE) [1, 2]. Developed method based on multi-objective nonlinear minimax optimization problem (MONMMOP) solution calculated by stochastic particles multi-swarm optimization algorithms (SPMSOA) from Pareto-optimal sat solutions taking into account binary preferences relationship [3].

PF MF simplest shielding method is EPS [13]. However, EPS does not provide the required shielding effectiveness. To implement necessary initial PF MF shielding factor, it is necessary used SAS [4–6]. Work [7] considered design issues of CES. But this CES designed in two-dimensional formulation. In this case, PF MF CES assumed in residential buildings central section. However, when MF shielding in residential buildings, it is necessary MF induction level reduced to safe level in apartments located in buildings edges. Most MF shielding research carried out based on two-dimensional MF modelling, which does not allow studying effectiveness decrease of original MF shielding in residential building edges [8]. This determines problem formulation and solution method for design of CES in TDM formulation. CES design reduction to geometric inverse magneto static problem (GIMSP) solution [3] and calculated as MONMMOP [16]. MONMMOP solution calculated by SPMSOA [12].

1. Definition of geometric forward magneto static problem for MF CES

Geometric forward magneto static problem (GFMSP) for OPL MF and for SW MF is MF calculated in any space point for given MF sources. MF mathematical modeling reduced to boundary value problem solution for electromagnetic field with known distribution of its sources in given area surface volume [11]. Maxwell equations describing electromagnetic fields in media with continuous or piecewise-continuously changing properties are basis for analytical and numerical modeling of any electromagnetic processes [1]. Considering electromagnetic processes model in following equations system

$$\mathrm{rot}\,\boldsymbol{H} = \boldsymbol{j} + \partial_t \boldsymbol{D} + \boldsymbol{j}_{ex} \tag{1}$$

$$\mathrm{rot}\,\boldsymbol{E} = -\partial_t \boldsymbol{B} \tag{2}$$

where $\boldsymbol{E}$ – electric field strength; $\boldsymbol{H}$ – magnetic field strength; $\boldsymbol{D}$ and $\boldsymbol{B}$ – electric and magnetic induction vectors; $\boldsymbol{j}$ – conductivity current density; $\boldsymbol{j}_{ex}$ – extraneous currents density created by sources located outside given area.

An intermediate position between constant and rapidly changing fields occupied by so-called quasi-stationary field, which is of particular importance in technical applications. A quasi-stationary field is electromagnetic field in which study displacement currents neglected in comparison with conduction

currents. When physical space includes conducting and non-conducting regions and infinitely distant points used quasi-static approximation [6]

$$\text{rot } \boldsymbol{H} = \boldsymbol{j} + \boldsymbol{j}_{ex} \tag{3}$$

$$\text{div } \mu\boldsymbol{H} = \text{div } \boldsymbol{B} = 0 \tag{4}$$

$$\text{rot } \boldsymbol{E} = -\partial_t \boldsymbol{B} \tag{5}$$

$$\text{div}\left(\varepsilon \boldsymbol{E}\right) = 0 \tag{6}$$

Another model used to describe an electromagnetic field that varies in time according to sinusoidal law [1]. Basic equations and methods for solving them significantly simplified by excluding one of independent variables – time – from consideration. When analyzing such problems symbolic method used and harmonically varying quantities written in form $A(x,t) = \hat{A}(x)e^{-i\omega t}$, where $\hat{A}(x)$ – is field complex amplitude. Using following notation Maxwell basic equations for vectors complex amplitudes of rapidly varying electromagnetic field when it changes harmonically in time:

$$\text{rot } \hat{\boldsymbol{H}} = \hat{\boldsymbol{j}} - i\omega\varepsilon\hat{\boldsymbol{E}} + \hat{\boldsymbol{j}}_{ex} \tag{7}$$

$$\text{rot } \hat{\boldsymbol{E}} = -i\omega\hat{\boldsymbol{B}} \tag{8}$$

$$div\left(\sigma\hat{\boldsymbol{E}} + \hat{\boldsymbol{j}}_{ex}\right) = i\omega\rho \tag{9}$$

When calculating current MF quasi-static approximation of Maxwell equations system is equivalent to Biot-Savart's law, which written in form [1]:

$$\boldsymbol{B}(P) = \frac{\mu_0 I_m}{4\pi}\int_L \frac{[d\boldsymbol{l}\times\boldsymbol{R}]}{\boldsymbol{R}^3} \tag{10}$$

where: $\boldsymbol{B}(P)$ – magnetic field induction at observation point P; $d\boldsymbol{l}$ – circuit element with current I_m; $\boldsymbol{R}$ – vector directed from contour element $d\boldsymbol{l}$ to observation point P.

Often, to simplify OPL MF mathematical mode, the phases wires taken in infinite long form and thin straight conductors, which allows two-dimensional MF model used which contains two spatial components along axes and does not depend on coordinate along which OPL wires conductors located. However, in this task, shielding winding (SW) vertical sections of active shielding system create significant projections of magnetic field intensity vector, which constitute, along coordinate, which determines three-dimensional magnetic field model used. Such model, in addition, also allows take into account MF intensity vector component along coordinate, created by OPL due to their sagging between supports.

Consider GFMSP solution for OPL MF mathematical model design. OPL wires position initially known. OPL wires instantaneous values currents set in dependences sinusoidal form. We set amplitudes A_i and phases φ_l of OPL PF wires currents. Consider OPL wire currents in complex form

$$I_i(t) = A_i \exp\, j(\omega t + \varphi_i) \tag{11}$$

Then, based on relation (10), initial MF induction $\boldsymbol{B}_0(P_i, \boldsymbol{I}_0(t), t)$ at point P created by OPL wires currents calculated in following form

$$\boldsymbol{B}_0(P_i, \boldsymbol{I}_0(t), t) = \sum_{l=1}^{L} \boldsymbol{B}_{0l}(P_i, I_l(t)) \tag{12}$$

OPL currents vector $\boldsymbol{I}_0$(t) introduced components of which are OPL wires currents

$$\mathbf{I}_0(t) = \{I_l(t)\}$$

Note that when OPL resulting MF calculating according to formula (16) for 3D modeling, it is necessary to take into account the real sagging of OPL wires, and elementary sections number of OPL conductors at ends of considered sections of OPL must be determined from required accuracy of resulting MF induction calculation, which generated by all OPL wires in given shielding space point.

Consider GFMSP for MF calculating generated by SW in shielding space points. Let us set SAS SW location coordinates geometric values vector, as well as SW currents amplitude A_i and phase φ_l [3]. Let's set SW currents in complex form

$$I_{ai}(t) = A_{ai} \exp\, j(\omega t + \varphi_{wi}) \tag{13}$$

Then, based on (13) similar to (12) MF induction in point P_i created by SW currents at time moment t calculated in following form

$$\boldsymbol{B}_y(P_i, \boldsymbol{I}_y(t), t) = \sum_{m=1}^{M} \boldsymbol{B}_{ym}(P_i, \boldsymbol{I}_{ym}(t), t) \tag{14}$$

here SW currents vector $\boldsymbol{I}_y(t)$ introduced with windings currents components $\boldsymbol{I}_y(t) = \{I_{ym}(t)\}$.

When calculating resulting MF generated by all SW wires, according to (14), for 3D modelling, it is necessary to take into account not only SW real dimensions of horizontal parts, but also real SW length since it is near ends of SW horizontal sections that greatest change in MF induction level generated by SW is observed. Naturally, that in 3D modeling in (14) it is necessary to take into account SW vertical parts, since it is these vertical parts that generate main part of the of MF induction level.

Then, based on superposition principle, the resulting magnetic field induction vector $\boldsymbol{B}(P_i, \boldsymbol{I}_0(t), \boldsymbol{I}_y(t), t)$ at the point P_i, created by power line wires currents (16) and SW windings currents is equal to vectors sum [3]

$$\boldsymbol{B}(P_i, \boldsymbol{I}_0(t), \boldsymbol{I}_y(t), t) = \boldsymbol{B}_0(P_i, \boldsymbol{I}_0(t), t) + \boldsymbol{B}_{\mathbf{y}}(P_i, \boldsymbol{I}_y(t), t) \tag{15}$$

2. Definition of GIMSP for MF CES design

GIMSP for MF CES design calculated of MF sources spatial location and MF parameters for generated compensating MF directed opposite to original MF [3]. Initial MF generated by OPL. Compensating MF simultaneously generated by SW of SAS and EPS. Consider desired parameters vector $\boldsymbol{X}$ for CES design with components are SAS SW geometric dimensions values vector $\boldsymbol{X_a}$, as well as SW currents A_{wi} and phases $\varphi_{\omega i}$: as well as EPS geometric dimensions vector $\boldsymbol{X_p}$, thickness and material [7]. Then, for given sought parameters vector $\boldsymbol{X}$ and uncertainty parameters vector $\boldsymbol{\delta}$ resulting MF induction effective value $\boldsymbol{B_R(X, \delta}, P_i)$ in shielding space point Q_i calculated based on finite element calculation system of COMSOL Multiphysics [7]. Then CES design reduced to MONMMOP [16]

$$\boldsymbol{B_R(X, \delta)} = \langle \boldsymbol{B_R(X, \delta}, P_i) \rangle \tag{16}$$

Vector nonlinear objective function (VNOF) $\boldsymbol{B_R(X, \delta}, P_i)$ are resulting MF induction effective values in all given shielding space points Pi. In this MONMMOP, it is necessary to calculated VNOF minimum along vector $\boldsymbol{X}$, but same VNOF maximum along the vector $\boldsymbol{\delta}$ [16].

At the same time, it is necessary to take into account desired parameters vector $\boldsymbol{X}$ restrictions in vector inequality and, possibly, vector equality form.

$$\boldsymbol{G}(\boldsymbol{X}) \le \boldsymbol{G}_{\max},\ \boldsymbol{H}(\boldsymbol{X}) = 0 \tag{17}$$

3. MONMMOP solution algorithm

VNOF (16) and vector constraints (17) are nonlinear functions of required parameters vector $\boldsymbol{X}$ and uncertainty parameters vector $\boldsymbol{\delta}$ calculated based on finite element system of COMSOL Multiphysics.

Consider calculation algorithm for Pareto-optimal solutions set of MONMMOP based on PMSOA [12].

To solve original MONMMOP (16) with constraints (17) PMSOA based on particle swarms set, which number is equal to VNOF components number. In this PMSOA particle i swarm j

movement described by following expressions [12]:

$$x_{ij}(t+1) = x_{ij}(t) + v_{ij}(t+1), \tag{18}$$

$$\delta_{ij}(t+1) = \delta_{ij}(t) + u_{ij}(t+1) \tag{19}$$

where

$$v_{ij}(t+1) = w_j v_{ij}(t) + c_{1j} r_{1j}(t) H(p_{1j} - \varepsilon_{1j}(t)) \left[y_{ij}(t) - x_{ij}(t) \right] + \ldots$$
$$\ldots + c_{2j} r_{2j}(t) H(p_{2j} - \varepsilon_{2j}(t)) \left[y_j^*(t) - x_{ij}(t) \right]$$
$$u_{ij}(t+1) = w_j u_{ij}(t) + c_{1j} r_{1j}(t) H(p_{1j} - \varepsilon_{1j}(t)) \left[z_{ij}(t) - \delta_{ij}(t) \right] + \ldots$$
$$\ldots + c_{2j} r_{2j}(t) H(p_{2j} - \varepsilon_{2j}(t)) \left[z_j^*(t) - \delta_{ij}(t) \right]$$

where $x_{ij}(t)$, $\delta_{ij}(t)$ and $v_{ij}(t)$, $u_{ij}(t)$ are position and velocity vectors components of the particle i of the swarm j.

Required parameters vector of original MONMMOP (16) presented in form of desired parameters vectors $\boldsymbol{X}$ and uncertainties parameters vectors $\boldsymbol{\delta}$. It is necessary to minimize VNOF (16) by parameters vectors $\boldsymbol{X}$ but maximize the same VNOF by uncertainty parameters vector $\boldsymbol{\delta}$. Therefore, each particle i of swarm j has two components of position $x_{ij}(t)$, $\delta_{ij}(t)$ and velocity $v_{ij}(t)$, $u_{ij}(t)$ for calculated two required vector $\boldsymbol{X}$ and vector $\boldsymbol{\delta}$.

To calculated global solution of original MONMMOP (16), during optimal solutions calculated individual swarms exchange information with each other. Particle i of swarm j at each motion step t binary preferences functions used. Solution $\boldsymbol{X}_j^*(t)$ calculated during VNOP function $\boldsymbol{B}(\boldsymbol{X}(t), P_j)$ optimization using swarm j is preferable to solution $\boldsymbol{X}_k^*(t)$ calculated during function $\boldsymbol{B}(\boldsymbol{X}(t), P_k)$ optimization using swarm k, i.e. if condition

$$\max_{i=1,m} \max_{\boldsymbol{\delta}} \boldsymbol{B}\left(P_i, \boldsymbol{X}_j^*(t), \boldsymbol{\delta}_j^*(t)\right) < \max_{i=1,m} \max_{\boldsymbol{\delta}} \boldsymbol{B}\left(P_i, \boldsymbol{X}_k^*(t), \boldsymbol{\delta}_k^*(t)\right) \tag{20}$$

Global optimal solution $\boldsymbol{X}_k^*(t)$ calculated by swarm k, global solution $\boldsymbol{X}_j^*(t)$ calculated by swarm j used, which is more preferable in relation to global solution $\boldsymbol{X}_k^*(t)$ calculated by swarm k based on preference relation (20).

Binary preference relations (20) considered for uncertainty parameters vector $\boldsymbol{\delta}$ worst value, at which corresponding MF induction values take maximum values, which corresponds to uncertainty parameters vector $\boldsymbol{\delta}$ greatest "harmfulness".

In conclusion, we note that many modern packages contain a large number of programs implementing various deterministic optimization algorithms. In particular, the Nelder-Mead and Levenberg-Marquardt algorithms (LMA) have become widespread. To improve convergence, second-order methods used, which the of objective function second derivatives – Hessian matrix used. Second-order algorithms, compared with first-order methods, allow for effective solution in a region close to optimal point, when gradient vector components have sufficiently small values. Such algorithms used in number of cases allows for optimal values calculating speed in extremum stationary region comparison with PSO.

Using Newton method iterative procedure for motion step d_k calculated reduced to linear system solving

$$H(B(x_k))d_k + J(B(x_k)) = 0 \tag{21}$$

Where Jacobian matrices J and Hessian matrices H components along vectors $\boldsymbol{X}$ to minimize VNUF (15) by parameters vectors $\boldsymbol{X}$ but along vectors $\boldsymbol{\delta}$ to maximize the same VNUF (15) by uncertainty parameters vector $\boldsymbol{\delta}$. Jacobian matrices J components calculated from particle i of swarm j movement velocities $v_{ij}(t)$ or $u_{ij}(t)$.

However, to calculate motion step d_k according to (21), it is necessary inverse Hessian matrices H calculated. That's why recently LMA have become widespread in quasi-Newton methods. Hessian matrix replaced to positive coefficient matrix and linear equations system used

$$J(B(x_k))J(B(x_k))^T d_k + \lambda_k d_k + \ldots$$
$$\ldots + J(B(x_k))B(x_k) = 0 \tag{22}$$

This resulting step d_k calculated from (22) used to particles movement to optimum calculated instead of (18)–(19).

The minimization and maximization process took place in 2 stages: at the first stage, 8 random initial points were selected, and the objective function was minimized by PSO. At second stage LMA used as 8 initial points for minimization. 8 points were selected for parallel calculation on 8 processor cores.

The calculation time ranged from 3 ms to 40 ms and was highly dependent on initial parameter values during PSO and optimal parameters calculating values desired accuracy.

4. Simulation results

Consider calculations results of resulting MF in designed CES. Figure 1 shown OPL, SAS and RBE diagram.

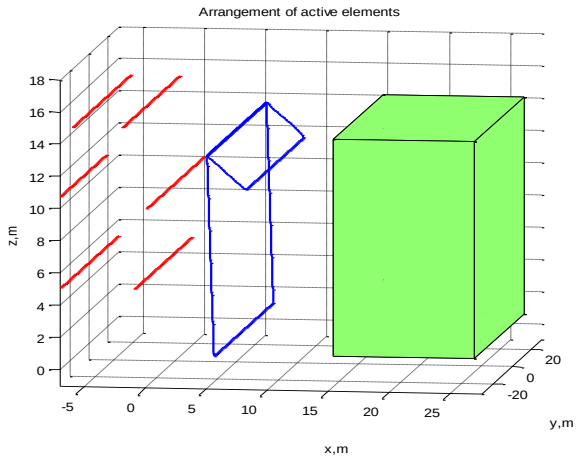

Fig. 1. OPL, SAS and RBE

Let us consider MF CES design of PF MF generated by two-circuit OPL in a five-story building.

Figure 2 shown resulting MF distribution along CES length for various coordinates along CES height.

Initial OPL PF MF level in RBE possibility by CES mean reduced to population safe level shown.

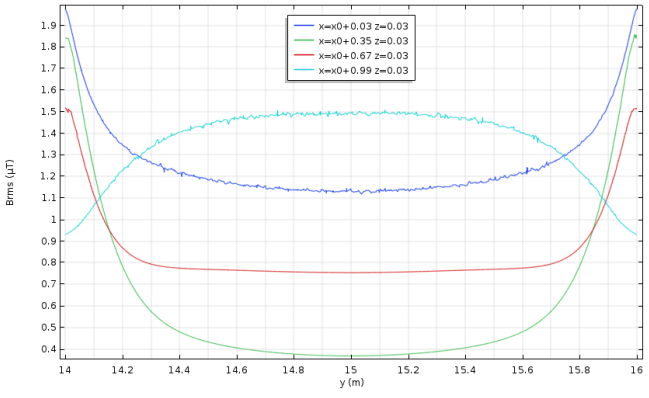

Fig. 2. Resulting MF

5. Experimental results

To conduct experimental studies CES prototype developed.

CES prototype includes a two-circuit OPL, two SAS SW and continuous EPS. OPL prototype phase wires coordinates given in Table 1.

Table 1. OPL prototype phase wires coordinates

Phases	*X*, m	*Z*, m
A1	-0.8638	0.6170
B1	-0.9872	1.2340
C1	-0.7404	1.8511
A2	-0.1234	0.617
B2	0	1.234
C2	-0.2468	1.8511

OPL Phases current: 30.851 amper.
OPL phase currents phase shifts:
Phases A: 0;
phases B: 2.0944 rad;
phases C: -2.0944 rad.
SAS SW prototype coordinates given in Table 2.

Table 2. SAS SW prototype coordinates

SAS SW	*X*, m	*Z*, m
SW1 top	1.2263	1.2503
SW1 bottom	0.7847	0.1737
SW2 top	0.8457	1.4927
SW2 bottom	1.0970	1.3482

SW1 current: 12.842 amper.
SW2 current : 41.232 amper.
SW1 phase currents phase shifts: 0.4573 rad.
SW2 phase currents phase shifts: 0.6576 rad.
SW length: 5.2 m. EPS length: 2 m.

Figure 3 shown CES prototype.

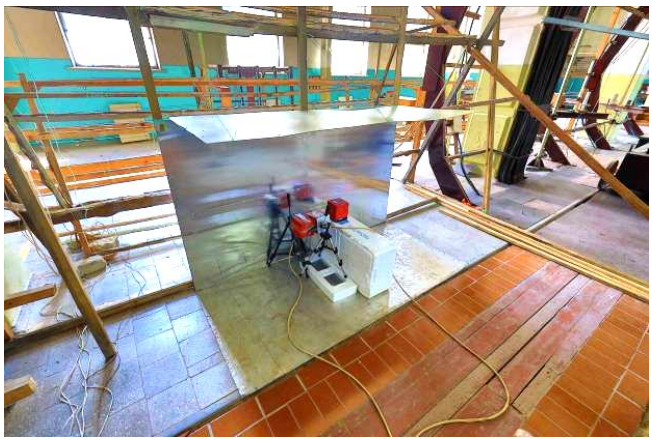

Fig. 3. CES prototype

During CES prototype experimental studies numerous measurements of initial MF parameters generated by OPL, resulting MF during EPS only operation, resulting MF during SAS only operation, resulting MF during SAS and EPS operation simultaneously – CES operation were carried out. As an example, Table 3 shows the results of experimental measurements of resulting MF during CES operation.

Figure 4 shown experimentally measured MF distributions along EPS length for various coordinates along EPS height and width.

Experimental measured resulting MF levels values coincided with calculated MF with 20% accuracy.

In conclusion, we note that results of calculating induction of resulting MF during CES operation largely determined by electrical conductivity value of EPS material adopted in calculation. Initially, when calculating the induction of resulting MF electrical conductivity value of EPS material taken from the reference book for aluminum adopted. However, experimental measurements of efficiency of initial MF shielding using EPS turned out to be significantly lower than calculated value.

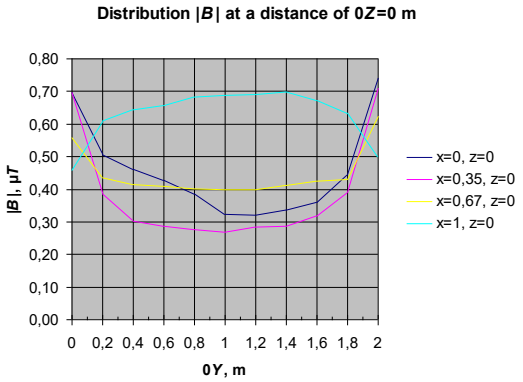

Fig. 4. Experimental measured resulting MF

Therefore, experimental measurements of electrical conductivity value of EPS material were carried out. As a result of these experimental measurements, it was established that actual electrical conductivity value of EPS material was an order of magnitude greater than value taken from the reference book for aluminum. Repeated calculation of resulting MF induction during CES operation with the experimentally determined electrical conductivity value of EPS material made it possible to reduce the discrepancy between calculated and experimentally measured values of resulting MF induction during CES operation to 20%.

6. Conclusions

1. Method for CES design based on stochastic MONMMOP solution for improvement OPL PF MF reduction effectiveness developed. CES consisted SAS and EPS and design based on resulting MF in RBE TDM.
2. MONMMOP solution calculated based on SPMSOA from Pareto-optimal sat solutions taking into account binary preferences relationship. VNOF calculated based on COMSOL Muliphysics package. Robustness of designed CES ensured by minimizing VNOF along desired parameters vector, but maximizing the same VNOF along uncertainty parameters vector.
3. TESR of CES based on TDM of resulting PF MF in RBE from OPL presented. Based on TESR possibility initial OPL PF MF level reduced to population safe level shown.

Table 3. Experimental measurements resulting MF during CES operation |B|, μT (distance of the protection zone along 0Z = 0 m)

Distance of the protection zone along 0*X*, *m*	Distance of the protection zone along 0Y, m										
	0	0.2	0.4	0.6	0.8	1	1.2	1.4	1.6	1.8	2
0	0.64	0.42	0.39	0.38	0.38	0.37	0.39	0.41	0.50	0.58	0.67
0.35	0.54	0.36	0.29	0.28	0.27	0.25	0.26	0.27	0.30	0.35	0.44
0.67	0.47	0.41	0.38	0.38	0.37	0.36	0.35	0.37	0.38	0.39	0.40
1	0.44	0.55	0.58	0.60	0.62	0.63	0.64	0.62	0.59	0.55	0.50

References

[1] Barsali S., Giglioli R., Poli D.: Active shielding of overhead line magnetic field: Design and applications. Electric Power Systems Research 110, 2014, 55–63 [https://doi.org/10.1016/j.epsr.2014.01.005].

[2] Bavastro D. et al.: Magnetic field mitigation at power frequency: design principles and case studies. IEEE Transactions on Industry Applications 51(3), 2015, 2009–2016 [https://doi.org/10.1109/tia.2014.2369813].

[3] Bravo-Rodríguez J., Del-Pino-López J., Cruz-Romero P.: A Survey on Optimization Techniques Applied to Magnetic Field Mitigation in Power Systems. Energies 12(7), 2019, 1332 [https://doi.org/10.3390/en12071332].

[4] Canova A. et al.: Active Shielding System for ELF Magnetic Fields. IEEE Transactions on Magnetics 51(3), 2015, 1–4 [https://doi.org/10.1109/tmag.2014.2354515].

[5] Canova A., Giaccone L.: High-performance magnetic shielding solution for extremely low frequency (ELF) sources. CIRED – Open Access Proceedings Journal 1, 2017, 686–690 [https://doi.org/10.1049/oap-cired.2017.1029].

[6] Canova A., Giaccone L.: Real-time optimization of active loops for the magnetic field minimization. International Journal of Applied Electromagnetics and Mechanics 56, 2018, 97–106 [https://doi.org/10.3233/jae-172286].

[7] Canova A., Giaccone L., Cirimele V.: Active and passive shield for aerial power lines. 25th International Conference on Electricity Distribution – CIRED 2019. Madrid 2019, 1096.

[8] Celozzi S.: Active compensation and partial shields for the power -frequency magnetic field reduction. IEEE International Symposium on Electromagnetic Compatibility. Minneapolis, USA, 1, 2002, 222–226 [https://doi.org/10.1109/isemc.2002.1032478].

[9] Del Pino Lopez J. C., Romero P. C.: Influence of different types of magnetic shields on the thermal behavior and ampacity of underground power cables. IEEE Transactions on Power Delivery 26(4), 2011, 2659–2667 [https://doi.org/10.1109/tpwrd.2011.2158593].

[10] Directive 2013/35/EU of the European Parliament and of the Council of 26 June 2013 on the minimum health and safety requirements regarding the exposure of workers to the risks arising from physical agents (electromagnetic fields) [http://data.europa.eu/eli/dir/2013/35/oj].

[11] Hasan G. T., Mutlaq A. H., Ali K. J.: The Influence of the Mixed Electric Line Poles on the Distribution of Magnetic Field. Indonesian Journal of Electrical Engineering and Informatics (IJEEI) 10(2), 2022, 292–301 [https://doi.org/10.52549/ijeei.v10i2.3572].

[12] Hashim F. A. et al.: Archimedes optimization algorithm: a new metaheuristic algorithm for solving optimization problems. Applied Intelligence 51(3), 2021, 1531–1551 [https://doi.org/10.1007/s10489-020-01893-z].

[13] Salceanu A., Paulet M., Alistar B. D., Asiminicesei O.: Upon the contribution of image currents on the magnetic fields generated by overhead power lines. International Conference on Electromechanical and Energy Systems (SIELMEN), 2019 [https://doi.org/10.1109/sielmen.2019.8905880].

[14] Sung H. et al.: Global Cancer Statistics 2020: GLOBOCAN Estimates of Incidence and Mortality Worldwide for 36 Cancers in 185 Countries. CA: A Cancer Journal for Clinicians 71(3), 2021, 209–249 [https://doi.org/10.3322/caac.21660].

[15] The International EMF Project. Radiation & Environmental Health Protection of the Human Environment World Health Organization. Geneva, Switzerland 2, 1996 [https://www.who.int/initiatives/the-international-emf-project].

[16] Ummels M.: Stochastic Multiplayer Games Theory and Algorithms. Amsterdam University Press, 2010.

Prof. D.Sc. Borys Kuznetsov
e-mail: kuznetsov.boris.i@gmail.com

Specialist in the field of automatic control systems. Laureate of the State Prize of Ukraine in the field of science and technology (2000). Since 2024, head of the department "Magnetism of Technical Objects" of the Institute of Power Machines and Systems named after A.M. Pidhorny of the NAS of Ukraine. Has 768 scientific papers, including 10 monographs and 6 textbooks, manages doctoral and postgraduate training.

https://orcid.org/0000-0002-1100-095X

Prof. D.Sc. Tatyana Nikitina
e-mail: tatjana55555@gmail.com

Specialist in the field of automatic control systems. Scientific research: multi-criteria synthesis of robust control of multi-mass electromechanical systems based on theoretical development and generalization of mathematical models and vector optimization methods. He has 357 scientific works, including a textbook, 3 study guides and 4 monographs.

https://orcid.org/0000-0002-9826-1123

Prof. D.Sc. Alexander Kutsenko
e-mail: oleksandr.kutsenko@khpi.edu.ua

A well-known scientist in the field of mathematical modeling and control processes of heat and power systems. Academician of the Academy of Sciences of the Higher School of Ukraine since 2017 in the scientific department of computer science and system analysis. Published over 160 scientific and educational and methodological works, author's certificates and patents. Scientific consultant of 5 dissertations for the degree of Doctor of Technical Sciences.

https://orcid.org/0000-0001-6059-3694

Ph.D. Ihor Bovdui
e-mail: ibovduj@gmail.com

Ihor Bovdui, Ph.D. (Eng.), is a senior research scientist at IPMach of NASU. Specialist in the field of designing passive/active shielding systems for object power energetics, control systems for electromechanical complexes and systems. Deputy head of the Department "Magnetism of Technical Objects" of the IPMach of the NASU. The total number of published scientific publications is 185, the number of educational and methodical works is 26.

https://orcid.org/0000-0003-3508-9781

Ph.D. Kostiantyn Chunikhin
e-mail: kvchunikhin@gmail.com

Kostiantyn Chunikhin, Ph.D. (Eng.), is a senior research scientist at IPMach of NASU. He holds a master's (2015) and Ph.D. (2020) from Kharkiv Polytechnic Institute. His research focuses on optimizing electromagnets for spacecraft control, predicting magnetic fields of elongated objects, and designing passive/active shielding systems for power lines. Author of 50 papers (28 in Scopus/WoS).

https://orcid.org/0000-0001-9822-5870

Ph.D. Olena Voloshko
e-mail: vinichenko.e.5@gmail.com

Olena Voloshko, Ph.D. (Eng.), is a research scientist at IPMach of NASU. She holds a Ph.D. (2013). Her research focuses on optimizing control algorithms for tracking systems, studying magnetic fields of industrial facilities, and designing active shielding systems for power lines. She is the author of over 52 scientific publications.

https://orcid.org/0000-0002-6931-998X

Ph.D. Eng. Roman Voliansky
e-mail: voliansky@ua.fm

He is the associate professor in the Department of Electromechanical Systems Automation and Electrical Drives of Igor Sikorsky Kyiv Politechnic University, Kyiv, Ukraine. His research area focuses on the use of control theory methods to study and design the motions of various regular and chaotic dynamical systems, control and optimization of electric drives under uncertainty by using sliding mode approach, numerical modelling and simulation, signal processing and analysis.

https://orcid.org/0000-0001-5674-7646

Ph.D. Viktoriia Ivannikova
e-mail: viktoriia.ivannikova@dcu.ie

Dr Viktoriia Ivannikova is an assistant professor at Dublin City University Business School. She holds a Ph.D. in Air Transportation Systems and has huge teaching and research experience in aviation. Her research focuses on airport operations and digital transformation in aviation. She is a member of several editorial boards, research committees and regular speaker at international conferences.

https://orcid.org/0000-0001-7967-4769